CrystEngComm

ROYAL SOCIETY OF CHEMISTRY

PAPER

View Article Online
View Journal | View Issue

Open Access Article. Published on 13 January 2025. Downloaded on 11/8/2025 3:24:16 AM.
This article is licensed under a Creative Commons Attribution-NonCommercial 3.0 Unported Licence.

Check for updates

Cite this: *CrystEngComm*, 2025, **27**, 1034

Mixed-ligand uranyl ion complexes with two flexible, pyridinium-based dicarboxylate zwitterions and simple anionic dicarboxylates†

Young Hoon Lee,[a] Youssef Atoini,[b] Sotaro Kusumoto,[c] Shinya Hayami,[d] Yang Kim,*[d] Jack Harrowfield *[e] and Pierre Thuéry *[f]

Received 17th December 2024,
Accepted 10th January 2025

DOI: 10.1039/d4ce01270d

rsc.li/crystengcomm

Two new dizwitterionic dicarboxylates, *E*-bis(*N*-(2′-carboxylatoethyl)pyridinium-4-yl)ethene (L1) and *E*-bis(3-carboxylatopyridiniomethyl)ethene (L2) have been reacted with uranyl nitrate hexahydrate under solvo-hydrothermal conditions, in the presence of dianionic dicarboxylates, yielding a series of 7 complexes which have been characterized by their crystal structure and luminescence properties. Both $[(UO_2)_2(L1)(1,2\text{-pda})_2]\cdot 2H_2O$ (**1**) and $[(UO_2)_2(L1)(1,4\text{-pda})_2]\cdot H_2O$ (**2**), where 1,2- and 1,4-pda^{2-} are 1,2- and 1,4-phenylenediacetates, crystallize as monoperiodic coordination polymers, either two-stranded and ladder-like or sinuous and daisychain-like, respectively. $[(UO_2)_2(L1)(t\text{-}1,4\text{-chdc})_2]$ (**3**), where *t*-1,4-chdc^{2-} is *trans*-1,4-cyclohexanedicarboxylate, is a diperiodic assembly with the **hcb** topology. *In situ* formation of oxalate anions (ox^{2-}) produces $[(UO_2)_2(L2)(ox)(OH)_2]$ (**4**), a diperiodic coordination polymer containing dihydroxo-bridged, dinuclear subunits. Simple chains are found in $[(UO_2)_2(L2)(pht)_2(H_2O)_2]\cdot 2H_2O$ (**5**), where pht^{2-} is phthalate, while $[(UO_2)_2(L2)(ipht)_2]\cdot 2H_2O\cdot 2CH_3CN$ (**6**), where ipht^{2-} is isophthalate, is another **hcb** network. In all these cases, each dicarboxylate ligand connects two metal centres. Finally, $[(UO_2)_2(L2)(t\text{-}1,4\text{-chdc})_2]$ (**7**) is a triperiodic framework with the unusual **mog** topology, in which *t*-1,4-chdc^{2-} is either bis(κ^2O,O'-chelating) or bis(μ_2-κ^1O:κ^1O'-bridging). Bond valence calculations reveal no very significant difference in donor strength between the two types of ligands. The importance of weak interactions (hydrogen bonding, π–π stacking) is discussed. Only complex **5** is strongly emissive in the solid state, with a photoluminescence quantum yield of 19%, and **6** is weakly emissive (4%), while **1**–**3** and **7** are non-emissive. The spectra of **5** and **6** display the usual vibronic fine structure, the peak positions being dependent on the uranyl ion equatorial environment.

Introduction

In our previous investigations of the use of carboxylate zwitterions as ligands of interest for the design of uranyl ion coordination polymers, notably mixed-ligand species,[1] the long-known tendency of the uranyl ion to form close-to-planar clusters and sheet-like coordination polymers[2–5] was a factor seemingly limiting our success in obtaining triperiodic systems. However, di- or trizwitterionic polycarboxylates of large size, particularly those based on double or triple pyridinium cores, allowed isolation of original architectures, such as mixed-ligand discrete rings,[6] cages,[7] polycatenated[8] and interpenetrated structures,[6,9] as well as showing some potential for the formation of anion-encapsulating cavities.[6,10] Flexibility allowing the ligands to adopt either convergent or divergent geometries for their coordination sites plays an essential part in the variety of structures which can be generated. In the ligands we have used previously, the two pyridinium rings were either linked to one another, flexibility being provided by the aliphatic chains bearing the carboxylate groups,[7,8] or they were attached to a central aromatic ring through flexible linkages.[6,8–11] We have now extended this work to two new dizwitterionic dicarboxylates presenting expected differences in conformational flexibility, which are also built on double pyridinium platforms and include a central linker containing a

[a] Department of Chemistry, University of Ulsan, Tekeunosaneop-ro 55beon-gil, Nam-gu, Ulsan 44610, Republic of Korea
[b] Technical University of Munich, Biogenic Functional Materials Group, Campus Straubing, Schulgasse 22, 94315 Straubing, Germany
[c] Department of Material & Life Chemistry, Kanagawa University, 3-27-1 Rokkakubashi, Kanagawa-ku, Yokohama 221-8686, Japan
[d] Department of Chemistry, Graduate School of Science and Technology, Institute of Industrial Nanomaterials (IINa), Kumamoto University, 2-39-1 Kurokami, Chuo-ku, Kumamoto 860-8555, Japan. E-mail: ykim@kumamoto-u.ac.jp
[e] Université de Strasbourg, ISIS, 8 allée Gaspard Monge, 67083 Strasbourg, France. E-mail: harrowfield@unistra.fr
[f] Université Paris-Saclay, CEA, CNRS, NIMBE, 91191 Gif-sur-Yvette, France. E-mail: pierre.thuery@cea.fr

† CCDC 2408741–2408747. For crystallographic data in CIF or other electronic format see DOI: https://doi.org/10.1039/d4ce01270d

This journal is © The Royal Society of Chemistry 2025

Open Access Article. Published on 13 January 2025. Downloaded on 11/8/2025 3:24:16 AM.
This article is licensed under a Creative Commons Attribution-NonCommercial 3.0 Unported Licence.

C═C double bond that introduces a measure of rigidity. In *E*-bis(*N*-(2′-carboxylatoethyl)pyridinium-4-yl)ethene (L1, Scheme 1(a)), the $-(CH_2)_2-COO^-$ terminal groups provide the required pliability. In contrast, *E*-bis(3-carboxylatopyridiniomethyl)ethene (L2, Scheme 1(a)) includes a longer $-(CH_2)-CH{=}CH-(CH_2)-$ central bridge, but the carboxylate groups are directly attached to the pyridinium rings. We have associated these ligands with various anionic dicarboxylates (Scheme 1(b)), 1,2- and 1,4-phenylenediacetates (1,2- and 1,4-pda^{2-}), phthalate and isophthalate (pht^{2-} and ipht^{2-}), *trans*-1,4-cyclohexanedicarboxylate (*t*-1,4-chdc^{2-}), and oxalate (ox^{2-}) to synthesize a series of seven neutral complexes which span the complete periodicity range. In particular, the combination of the aliphatic dicarboxylate *t*-1,4-chdc^{2-} with L2 has led to the isolation of a triperiodic framework.

Experimental

Synthesis

Caution! Uranium is a radioactive and chemically toxic element, and uranium-containing samples must be handled with suitable care and protection. Small quantities of reagents and solvents were employed to minimize any potential hazards arising both from the presence of uranium and the use of pressurized vessels for the syntheses.

$[UO_2(NO_3)_2(H_2O)_2]\cdot 4H_2O$ (RP Normapur, 99%) was purchased from Prolabo; 1,2- and 1,4-phenylenediacetic acids (1,2- and 1,4-pdaH$_2$), phthalic and isophthalic acids (phtH$_2$ and iphtH$_2$) were from Aldrich, and *trans*-1,4-cyclohexanedicarboxylic acid (*t*-1,4-chdcH$_2$) was from Alfa-Aesar. For all syntheses of complexes, the solutions were placed in 10 mL tightly closed glass vessels (Pyrex culture tubes with SVL15 stoppers and Teflon-coated seals, provided by VWR) and heated at 140 °C in a sand bath (Harry Gestigkeit ST72). The crystals were grown in the hot, pressurized solutions and not as a result of a final return to ambient conditions.

L1H$_2$Cl$_2$. The precursor to the ligand L1 was prepared by a minor modification of a literature method.[12] A mixture of 1,2-di(4-pyridyl)ethylene (15 mmol) and acrylic acid (30 mL, 50-fold molar excess) was stirred in chloroform (20 mL) at ambient temperature for 2 days. After this time, acetone–HCl (6 : 1, 15 mL) was added to the mixture, resulting in a light yellow precipitate that was subsequently collected by filtration. The product was washed with acetone and dried in the air (yield: 80%).

L2H$_2$Br$_2$. The precursor to the ligand L2 was prepared by a minor modification again of a literature method.[13] *trans*-1,4-Dibromo-2-butene (10 mmol) and ethyl nicotinate (50 mmol) were mixed in acetonitrile (50 mL) and heated at reflux for 2 days. After cooling to ambient temperature, the precipitate formed was collected by filtration, and dried in the air. It was then dissolved in 5% (w/v) HBr (50 mL) and heated at reflux for 5 hours. After evaporation under reduced pressure, the product was washed with acetone, resulting in a pale pink powder (yield: 41%).

$[(UO_2)_2(L1)(1,2\text{-pda})_2]\cdot 2H_2O$ (1). L1H$_2$Cl$_2$ (20 mg, 0.05 mmol), 1,2-pdaH$_2$ (20 mg, 0.10 mmol), and $[UO_2(NO_3)_2(H_2O)_2]\cdot 4H_2O$ (25 mg, 0.05 mmol) were dissolved in a mixture of water (0.6 mL) and *N*,*N*-dimethylacetamide (0.2 mL). Yellow crystals of complex **1** were obtained in low yield within two days.

$[(UO_2)_2(L1)(1,4\text{-pda})_2]\cdot H_2O$ (2). L1H$_2$Cl$_2$ (20 mg, 0.05 mmol), 1,4-pdaH$_2$ (20 mg, 0.10 mmol), and $[UO_2(NO_3)_2(H_2O)_2]\cdot 4H_2O$ (25 mg, 0.05 mmol) were dissolved in a mixture of water (0.6 mL) and acetonitrile (0.2 mL). Yellow crystals of complex **2** were obtained in low yield within three weeks.

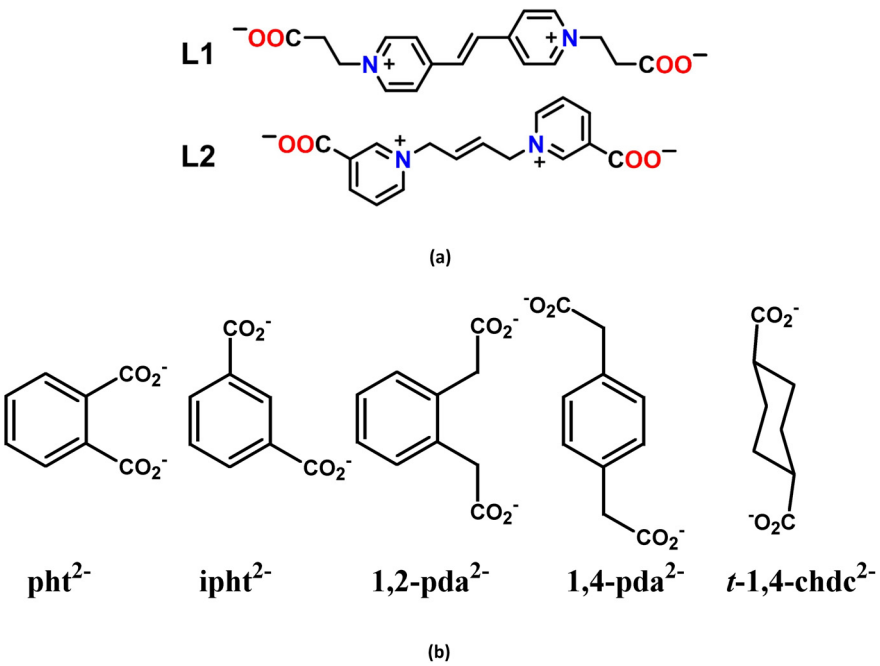

Scheme 1 (a) The dizwitterionic dicarboxylates L1 and L2. (b) The dicarboxylate coligands employed.

Open Access Article. Published on 13 January 2025. Downloaded on 11/8/2025 3:24:16 AM.
This article is licensed under a Creative Commons Attribution-NonCommercial 3.0 Unported Licence.

[$(UO_2)_2$(L1)(*t*-1,4-chdc)$_2$] (3). $L1H_2Cl_2$ (20 mg, 0.05 mmol), *t*-1,4-chdcH_2 (9 mg, 0.05 mmol), and $[UO_2(NO_3)_2(H_2O)_2]\cdot 4H_2O$ (25 mg, 0.05 mmol) were dissolved in a mixture of water (0.6 mL) and acetonitrile (0.2 mL). Yellow crystals of complex **3** were obtained in low yield overnight.

[$(UO_2)_2$(L2)(ox)(OH)$_2$] (4). $L2H_2Br_2$ (24 mg, 0.05 mmol), CsI (26 mg, 0.10 mmol), and $[UO_2(NO_3)_2(H_2O)_2]\cdot 4H_2O$ (25 mg, 0.05 mmol) were dissolved in a mixture of water (0.6 mL) and acetonitrile (0.2 mL). Yellow crystals of complex **4** were obtained in low yield within three days. The same complex was obtained with CsI replaced by 1,3-phenylenediacetic, camphoric, or pimelic acid.

[$(UO_2)_2$(L2)(pht)$_2$(H_2O)$_2$]·2H_2O (5). $L2H_2Br_2$ (24 mg, 0.05 mmol), phtH_2 (9 mg, 0.05 mmol), and $[UO_2(NO_3)_2(H_2O)_2]\cdot 4H_2O$ (25 mg, 0.05 mmol) were dissolved in a mixture of water (0.6 mL) and acetonitrile (0.2 mL). Yellow crystals of complex **5** were obtained in low yield overnight.

[$(UO_2)_2$(L2)(ipht)$_2$]·2H_2O·2CH_3CN (6). $L2H_2Br_2$ (24 mg, 0.05 mmol), iphtH_2 (9 mg, 0.05 mmol), and $[UO_2(NO_3)_2(H_2O)_2]\cdot 4H_2O$ (25 mg, 0.05 mmol) were dissolved in a mixture of water (0.6 mL) and acetonitrile (0.2 mL). Yellow crystals of complex **6** were obtained in low yield overnight.

[$(UO_2)_2$(L2)(*t*-1,4-chdc)$_2$] (7). $L2H_2Br_2$ (24 mg, 0.05 mmol), *t*-1,4-chdcH_2 (9 mg, 0.05 mmol), and $[UO_2(NO_3)_2(H_2O)_2]\cdot 4H_2O$ (25 mg, 0.05 mmol) were dissolved in a mixture of water (0.6 mL) and *N*,*N*-dimethylacetamide (0.2 mL). Yellow crystals of complex **7** were obtained in low yield overnight.

Crystallography

Data collections were performed at 100(2) K on a Bruker D8 Quest diffractometer using an Incoatec Microfocus Source (IμS 3.0 Mo) and a PHOTON III area detector, and operated with APEX4.[14] The data were processed with SAINT,[15] and empirical absorption corrections were made with SADABS.[16,17] The structures were solved by intrinsic phasing with SHELXT,[18] and refined by full-matrix least-squares on F^2 with SHELXL,[19] using the ShelXle interface.[20] When present, the hydrogen atoms bound to oxygen atoms were retrieved from residual electron density maps and they were refined with geometric restraints. All other hydrogen atoms in all compounds were introduced at calculated positions and treated as riding atoms with an isotropic displacement parameter equal to 1.2 times that of the parent atom (1.5 for CH_3). In **2**, the water molecule is too close to its image by inversion and it has been given an occupancy factor of 0.5 accordingly. In **5**, part of the zwitterionic ligand is disordered over two positions which have been refined with occupancy parameters constrained to sum to unity and restraints on bond lengths and displacement parameters; only part of the disorder of the aromatic ring could be resolved. For compounds **2**, **3**, and **6**, the SQUEEZE[21] software was used to subtract the contribution of disordered solvent molecules to the structure factors, the number of electrons added corresponding to approximately 2, 1 and 0.5 water molecules per formula unit, respectively. Crystal data and structure refinement parameters are given in Table 1. Drawings were made with ORTEP-3,[22,23] and VESTA.[24] The topological analyses were done with ToposPro.[25]

Luminescence measurements

Emission spectra were recorded on solid samples using an Edinburgh Instruments FS5 spectrofluorimeter equipped with a 150 W CW ozone-free xenon arc lamp, dual-grating excitation and emission monochromators (2.1 nm mm^{-1} dispersion; 1200 grooves per mm) and an R928P photomultiplier detector. The

Table 1 Crystal data and structure refinement details

	1	2	3	4	5	6	7
Chemical formula	$C_{38}H_{38}N_2O_{18}U_2$	$C_{38}H_{36}N_2O_{17}U_2$	$C_{34}H_{38}N_2O_{16}U_2$	$C_{18}H_{16}N_2O_{14}U_2$	$C_{32}H_{30}N_2O_{20}U_2$	$C_{36}H_{32}N_4O_{18}U_2$	$C_{32}H_{34}N_2O_{16}U_2$
M/g mol^{-1}	1286.76	1268.75	1206.72	960.39	1238.64	1284.71	1178.67
Crystal system	Triclinic	Monoclinic	Triclinic	Monoclinic	Triclinic	Triclinic	Triclinic
Space group	$P\bar{1}$	$P2_1/c$	$P\bar{1}$	$P2_1/n$	$P\bar{1}$	$P\bar{1}$	$P\bar{1}$
a/Å	8.1663(3)	11.2350(4)	8.7832(4)	9.7403(5)	8.4515(3)	8.3083(3)	8.8565(2)
b/Å	10.5584(3)	13.3313(5)	9.7665(5)	10.6942(5)	10.5811(4)	9.7524(3)	9.0719(3)
c/Å	12.5335(4)	14.3587(5)	11.6623(6)	10.9139(5)	10.5850(3)	13.3763(5)	11.6001(3)
α/°	100.8155(12)	90	76.391(2)	90	75.8824(11)	99.2243(17)	73.5981(9)
β/°	91.1157(13)	109.3383(16)	83.846(2)	96.3201(19)	72.1083(12)	100.6840(18)	86.2684(9)
γ/°	111.4308(12)	90	81.044(2)	90	75.7896(14)	108.6144(16)	68.7753(9)
V/Å^3	983.50(6)	2029.27(13)	957.87(8)	1129.93(9)	858.55(5)	980.89(6)	832.72(4)
Z	1	2	1	2	1	1	1
Reflections collected	47 714	112 330	67 502	94 664	45 194	61 474	53 583
Independent reflections	5986	3855	3636	3448	5208	3717	5059
Observed reflections [$I > 2\sigma(I)$]	5596	3825	3536	3395	5005	3591	4890
R_{int}	0.045	0.048	0.051	0.046	0.040	0.044	0.048
Parameters refined	277	277	244	167	322	278	235
R_1	0.020	0.032	0.046	0.019	0.021	0.022	0.018
wR_2	0.052	0.075	0.119	0.047	0.052	0.057	0.043
S	1.058	1.349	1.231	1.126	1.114	1.118	1.118
$\Delta\rho_{min}$/e Å^{-3}	−1.16	−1.57	−2.41	−1.05	−2.51	−0.71	−1.33
$\Delta\rho_{max}$/e Å^{-3}	1.75	1.43	4.14	2.57	1.84	2.78	1.80

Open Access Article. Published on 13 January 2025. Downloaded on 11/8/2025 3:24:16 AM.
This article is licensed under a Creative Commons Attribution-NonCommercial 3.0 Unported Licence.

powdered compounds were pressed to the wall of a quartz tube, and the measurements were performed using the right-angle mode in the SC-05 cassette. An excitation wavelength of 420 nm was used in all cases and the emission was monitored from 450 to 640 nm. The quantum yield measurements were performed using a Hamamatsu Quantaurus C11347 absolute photoluminescence quantum yield spectrometer and exciting the samples between 300 and 400 nm.

Results and discussion

Syntheses

All complexes in the present series were obtained in rather low yield, an observation that may simply mean that they are of relatively high solubility in the reaction media used but also may be due to the instability of the zwitterionic ligands under the same conditions. That the latter may be the case, at least with L2, is indicated by the isolation of complex **4** in the presence of CsI, where the oxalate present could only originate from the zwitterion. It is possible that I_2 formed by nitrate oxidation of iodide could facilitate oxalate formation but this seems to be excluded by the isolation of the same complex when CsI is replaced by various carboxylic acids. Once again, it is only possible to speculate as to the solution chemistry which may lead to the isolated crystals.

Crystal structures

The uranyl cation in the complex $[(UO_2)_2(L1)(1,2\text{-pda})_2]\cdot 2H_2O$ (**1**) is κ^2O,O'-chelated by one centrosymmetric L1 and two 1,2-pda^{2-} ligands (Fig. 1), this being a mode relatively uncommon for a dizwitterionic ligand,[1] which gives a hexagonal-bipyramidal uranium environment [U–O(oxo), 1.772(2) and 1.778(2) Å; U–O(carboxylato), 2.448(2)–2.5131(19) Å]. The two longest U–O bonds are those formed with L1, thus seemingly confirming the trend for zwitterionic carboxylates to be somewhat weaker donors than anionic carboxylates, as previously noted.[1] Bond valence parameters (BVs)[26] calculated with PLATON[27] (Table 2) provide a convenient means of quantifying this effect. Both ligands have divergent donor groups, with the carboxylate groups of L1 divergently oriented approximately perpendicular to the bis(4-pyridyl)ethene plane, and the coordination polymer formed is monoperiodic and directed along [100]. The chains are double-stranded or ladderlike, with two UO_2(1,2-pda) rows cross-linked by linear L1 ligands. The chains are arranged into layers parallel to (011) and they are interdigitated, with interlayer, parallel-displaced π–π interactions involving 1,2-pda^{2-} and L1 [centroid⋯centroid distance, 3.9553(18) Å; dihedral angle, 11.43(15)°; slippage, 2.04 Å]. The Kitaigorodsky packing index (KPI, evaluated with PLATON) of 0.72 indicates a compact arrangement.

Replacement of 1,2- by 1,4-pda^{2-} gives the complex $[(UO_2)_2(L1)(1,4\text{-pda})_2]\cdot H_2O$ (**2**) in which the uranium atom is also in a hexagonal-bipyramidal environment formed by one centrosymmetric, zwitterionic and two anionic ligands [U–O(oxo), 1.777(4) and 1.780(5) Å; U–O(carboxylato), 2.429(5)–2.516(4) Å] (Fig. 2). However, in contrast to **1**, the ligand L1 has

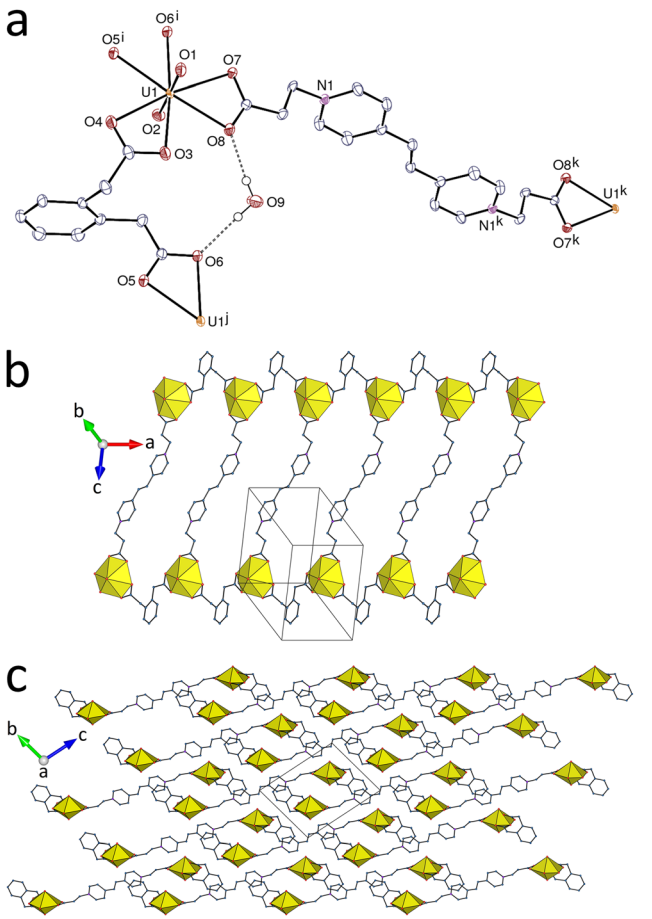

Fig. 1 (a) View of complex **1** with displacement ellipsoids shown at the 50% probability level. Carbon-bound hydrogen atoms are omitted and hydrogen bonds are shown as dashed lines. Symmetry codes: i = *x* − 1, *y*, *z*; j = *x* + 1, *y*, *z*; k = 1 − *x*, 2 − *y*, −*z*. (b) The two-stranded monoperiodic coordination polymer with uranium coordination polyhedra in yellow. (c) Packing with chains viewed end-on.

here both the longest and the shortest of the U–O bonds, resulting in very large standard deviations in mean bond length and BV values which make the difference between BV_{AC} and BV_{ZI} insignificant (Table 2). Obviously, the variation of donor strength of the two ligands is sufficiently small to be masked by other small contributions due to weak interactions. The 1,4-pda^{2-} ligand assumes a convergent shape, so that 22-membered, $[UO_2(1,4\text{-pda})]_2$ rings are formed, which are further assembled by the divergent L1 ligands into a daisychain-like monoperiodic polymer directed along [201]. The same rings have been found in various other uranyl ion complexes of 1,4-pda^{2-},[28–30] indicating that this may be the dominant factor determining the structure. Here, they are stabilized by the inclusion of a disordered water molecule involved in OH⋯O hydrogen bonds to the carboxylate oxygen atoms O4 and O5 pertaining to the dinuclear ring [O⋯O, 2.988(10) and 2.982(10) Å; O–H⋯O, 167(6) and 130(7)°], thus giving a hydrogen bonding ring with the graph set descriptor[31] $R_2^2(13)$, and also in a CH⋯O interaction involving an L1 methylene group in a neighbouring chain. As seen when viewed down the *a* axis, these chains have

Open Access Article. Published on 13 January 2025. Downloaded on 11/8/2025 3:24:16 AM.
This article is licensed under a Creative Commons Attribution-NonCommercial 3.0 Unported Licence.

Table 2 Mean U–O bond lengths (Å) and bond valence parameters in complexes **1**–**7**[a]

Complex	CN[b]	U–O_{oxo}	U–O_{AC} (monodentate)	U–O_{AC} (chelating)[c]	U–O_{ZI} (monodentate)	U–O_{ZI} (chelating)[c]	BV_{AC}[d] (monodentate)	BV_{AC}[d] (chelating)[c]	BV_{ZI}[d] (monodentate)	BV_{ZI}[d] (chelating)[c]
1	8	1.775(3)		2.458(7)		2.497(16)		0.451(6)		0.418(14)
2	8	1.7785(15)		2.46(3)		2.47(4)		0.45(3)		0.44(4)
3	8	1.776(9)		2.46(2)		2.460(4)		0.452(18)		0.449(4)
4	7	1.789(4)	2.469(5)		2.339(2)		0.441(4)		0.567	
5	7	1.774(4)	2.368(15)		2.368(2)		0.538(16)		0.536	
6	8	1.7765(15)		2.467(9)		2.50(5)		0.443(8)		0.42(4)
7	7	1.775(4)	2.390(6)	2.4373(6)	2.3080(18)		0.515(7)	0.4690(10)	0.604	

[a] The esds on mean values measure the dispersion of individual values; no esd is given for single BV values. [b] CN, coordination number. [c] The term "chelating" refers here only to κ^2O,O'-chelating species, not to those forming 5- or 7-membered chelate rings. [d] BV_{AC}, mean bond valence parameter for anionic carboxylates, BV_{ZI}, mean bond valence parameter for zwitterionic carboxylates.

a very sinuous shape and are tightly stacked (KPI, 0.69), with a possible interchain parallel-displaced π–π interaction involving 1,4-pda^{2-} and L1 [centroid···centroid distance, 3.939(5) Å; dihedral angle, 17.2(4)°; slippage, 1.40 Å]. However, this interaction does not appear as exceeding dispersion on the Hirshfeld surface (HS),[32,33] which does, however, provide evidence of CH···O hydrogen bonds between L1 and one uranyl oxo group, a factor which serves both to knit the polymer strands into a tridimensional array and to orient aromatic rings into proximity, possibly preventing formation of a simple sheet-like form.

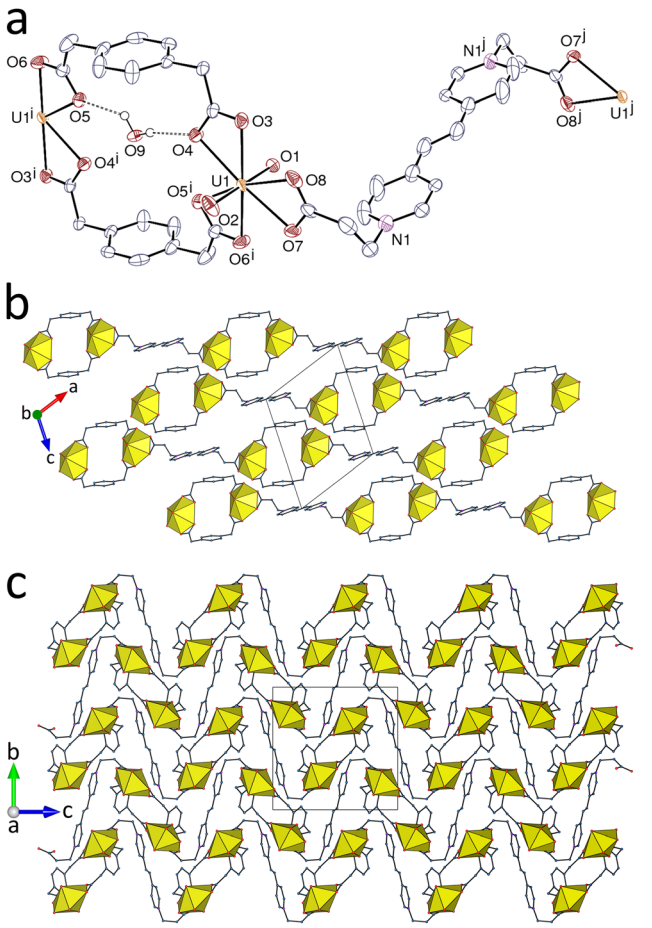

Fig. 2 (a) View of complex **2** with displacement ellipsoids shown at the 50% probability level. Carbon-bound hydrogen atoms are omitted and hydrogen bonds are shown as dashed lines. Symmetry codes: i = −*x*, 1 − *y*, 1 − *z*; j = 2 − *x*, 1 − *y*, 2 − *z*. (b) Arrangement of monoperiodic coordination polymers parallel to (010). (c) Packing with chains viewed edge-on.

Tris-chelation of uranyl by one zwitterionic and two anionic ligands, all centrosymmetric, is also found in the complex [$(UO_2)_2$(L1)(*t*-1,4-chdc)$_2$] (**3**), shown in Fig. 3 [U–O(oxo), 1.767(7) and 1.785(8) Å; U–O(carboxylato), 2.442(7)–2.495(6) Å]. The longest bond here is with atom O6 from *t*-1,4-chdc^{2-}, the next two being those with L1, so that the mean BV values are not different (Table 2). The two centrosymmetric *t*-1,4-chdc^{2-} ligands differ by the orientation of the carboxylate groups, which are both axial in the ligand containing O3 and O4 and equatorial in the case of O5 and O6 (the diequatorial conformation being generally more common in metal complexes[34]). In contrast to the monoperiodic coordination polymers found in **1** and **2**, that formed here is diperiodic and parallel to (1$\bar{2}$2). It has the {6^3} point symbol and the **hcb** topological type, a very common occurrence in complexes in which the uranyl ion is tris-chelated by three divergent dicarboxylate ligands. The hexanuclear cells are however very far from the regular hexagonal geometry, the L1 ligand having an S-shape. A methylene group of L1 is involved in a hydrogen bond with a uranyl oxo group, but there is no π–π interaction of L1, and the KPI of 0.67 indicates that only small solvent-accessible voids are present (see Experimental).

The complex [$(UO_2)_2$(L2)(ox)(OH)$_2$] (**4**) was obtained in the presence of different additional reagents, CsI, 1,3-phenylenediacetic, camphoric, or pimelic acid (albeit always in extremely low yield), thus suggesting that oxalate is produced through oxidation of L2. Oxalate formation during solvothermal processes is frequently observed,[35–40] and nitrate has been shown in several cases[36,39] to be the oxidant involved. The uranyl cation in **4** is chelated by one centrosymmetric ox^{2-} ligand forming a 5-membered ring, and it is also bound to one monodentate carboxylate group from the centrosymmetric ligand L2 and two hydroxide anions, the uranium environment being pentagonal-bipyramidal (Fig. 4) [U–O(oxo), 1.784(2) and 1.793(2) Å; U–O(carboxylato), 2.339(2)–2.473(2) Å; U–

Open Access Article. Published on 13 January 2025. Downloaded on 11/8/2025 3:24:16 AM.
This article is licensed under a Creative Commons Attribution-NonCommercial 3.0 Unported Licence.

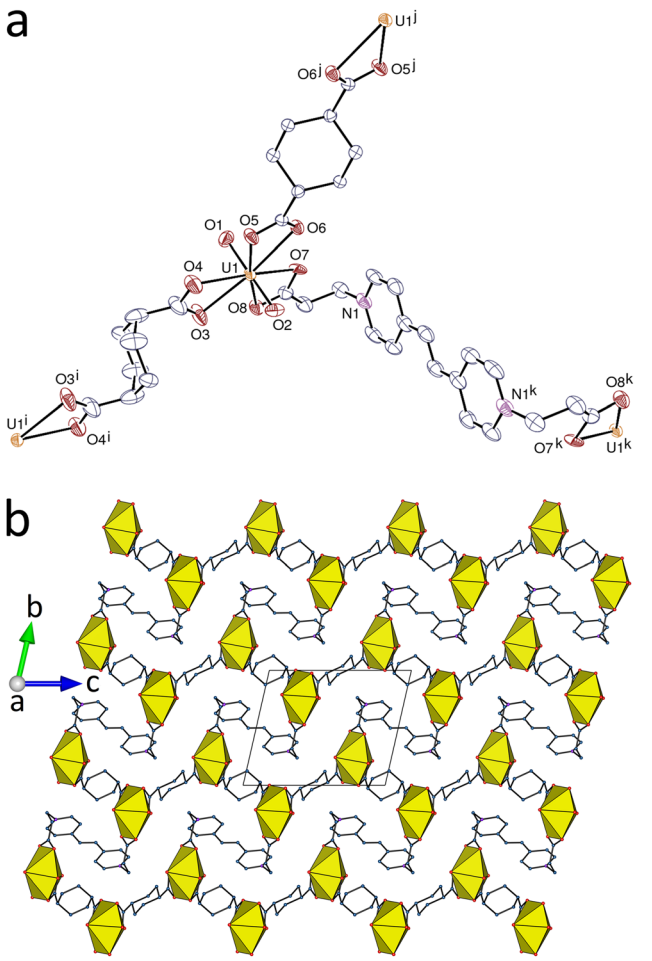

Fig. 3 (a) View of compound **3** with displacement ellipsoids shown at the 40% probability level and hydrogen atoms omitted. Symmetry codes: i = 2 − *x*, 2 − *y*, −*z*; j = −*x*, 2 − *y*, 1 − *z*; k = −*x*, 1 − *y*, −*z*. (b) View of the **hcb** diperiodic coordination polymer.

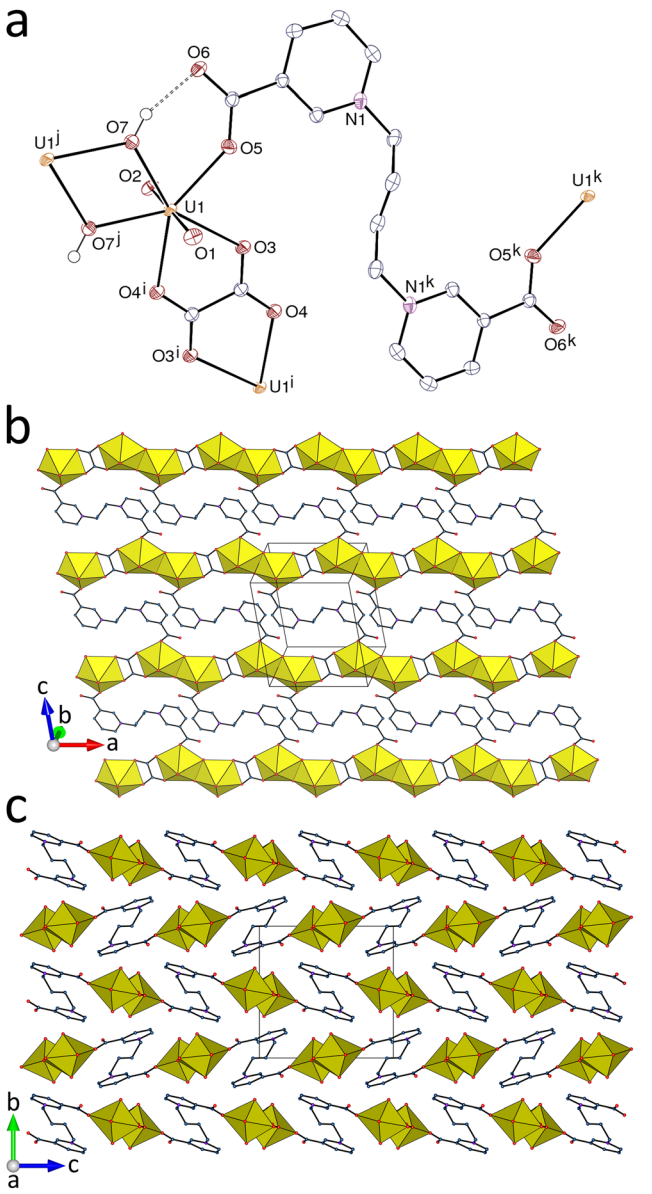

Fig. 4 (a) View of compound **4** with displacement ellipsoids shown at the 50% probability level. Carbon-bound hydrogen atoms are omitted and the hydrogen bond is shown as a dashed line. Symmetry codes: i = 1 − *x*, 1 − *y*, −*z*; j = 2 − *x*, 1 − *y*, −*z*; k = 1 − *x*, 1 − *y*, 1 − *z*. (b) The diperiodic coordination polymer. (c) Packing with layers viewed edge-on.

O(hydroxido), 2.279(2) and 2.348(2) Å]. The shortest U–O(carboxylato) bond here is that with L2 (Table 2), this being probably due to the constrained geometry of oxalate bonding. The hydroxo (instead of oxo) nature of O7 is confirmed by its overall bond valence parameter of 1.2. The L2 ligand assumes an S-shape and is divergent, both ligands being simple links. The double hydroxide bridges result in the formation of uranyl dimers with edge-sharing coordination polyhedra, these dimers being further assembled into linear chains running along the *a* axis by the oxalate links. These rows are cross-linked by the L2 ligands to give a diperiodic polymer parallel to (010). If the dimers are considered as 4-coordinated (4-c) nodes, the topological type is the usual **sql**. The hydroxide anion forms a strong hydrogen bond with the uncoordinated carboxylate atom O6 [O···O, 2.742(3) Å; O–H···O, 159(4)°], thus building an $R_1^1(6)$ ring. The L2 ligands are not involved in any π–π interaction, but two CH···O interactions involving both uranyl oxo groups are present, one with an aromatic CH group within the layers and the other with a methylene group in the adjoining layer [C···O, 3.105(4) and 3.411(4) Å; C–H···O, 130 and 156°]. In addition to CH···O(uranyl) hydrogen bonds, one U═O···π(pyridinium) interaction involving a neighbouring layer is also apparent on the HS, as previously found in comparable systems.[41] The KPI of 0.73 reveals no solvent-accessible space.

Phthalate is a convergent ligand and, as expected, it forms a 7-membered chelate ring in $[(UO_2)_2(L2)(pht)_2(H_2O)_2]\cdot 2H_2O$ (**5**), shown in Fig. 5. While one of its carboxylate groups is monodentate, the other is bridging in the *syn*/*anti* μ_2-κ^1O:κ^1O' mode. The uranium pentagonal-bipyramidal environment is completed by one monodentate carboxylate group from the extended, centrosymmetric L2, and one water molecule [U–O(oxo), 1.770(2) and 1.777(2) Å; U–O(carboxylato), 2.357(2)–2.389(2) Å; U–O(water), 2.450(2) Å]. The bond length with L2 is

Open Access Article. Published on 13 January 2025. Downloaded on 11/8/2025 3:24:16 AM.
This article is licensed under a Creative Commons Attribution-NonCommercial 3.0 Unported Licence.

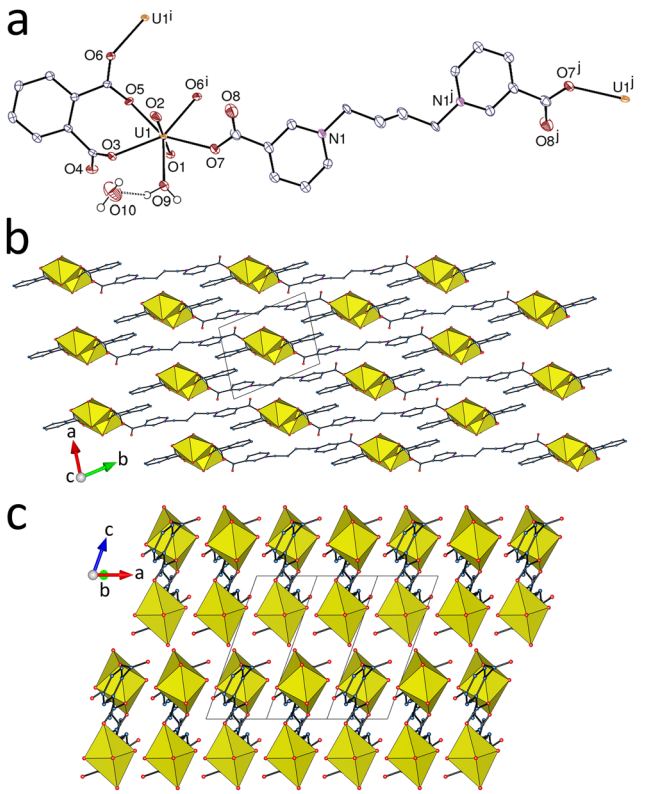

Fig. 5 (a) View of compound **5** with displacement ellipsoids shown at the 50% probability level. Only one position of the disordered parts is represented. Carbon-bound hydrogen atoms are omitted and the hydrogen bond is shown as a dashed line. Symmetry codes: i = 1 − *x*, 1 − *y*, −*z*; j = −*x*, 3 − *y*, −*z*. (b) Packing with chains viewed edge-on. (c) Packing with chains viewed end-on.

within the range of those with the anionic ligand (Table 2), so that no difference in donor strength is obvious here. The uranium atom is a 3-c node and both ligands are simple edges, and the coordination polymer formed is monoperiodic and directed along [1$\bar{2}$0], with centrosymmetric dimers with double pht^{2-} bridges being connected through L2 ligands. The packing (KPI, 0.75) involves a single parallel-displaced π–π interaction between pht^{2-} and L2 [centroid⋯centroid distance, 3.969(10) Å; dihedral angle, 5.5(8)°; slippage, 2.06 Å].

Replacing pht^{2-} by its divergent positional isomer $ipht^{2-}$ gives the complex $[(UO_2)_2(L2)(ipht)_2]\cdot 2H_2O\cdot 2CH_3CN$ (**6**), in which the uranyl cation is tris(κ^2*O*,*O*′-chelated) by one S-shaped L2 and two $ipht^{2-}$ ligands, all centrosymmetric, resulting in a hexagonal-bipyramidal uranium coordination polyhedron [U–O(oxo), 1.775(3) and 1.778(3) Å; U–O(carboxylato), 2.448(3)–2.549(3) Å] (Fig. 6). As L1 in complex **2**, L2 is associated with both the shortest and longest equatorial bonds, with the consequence that, here also, no significant difference in donor strength between the two ligands is apparent (Table 2). With the uranium atom as a 3-c node and all ligands as edges, the diperiodic coordination polymer formed, parallel to (1$\bar{2}\bar{3}$), has the **hcb** topological type. The sheets are nearly planar and each elongated hexanuclear cell contains two acetonitrile molecules with their nitrogen atoms within the layer plane and involved in

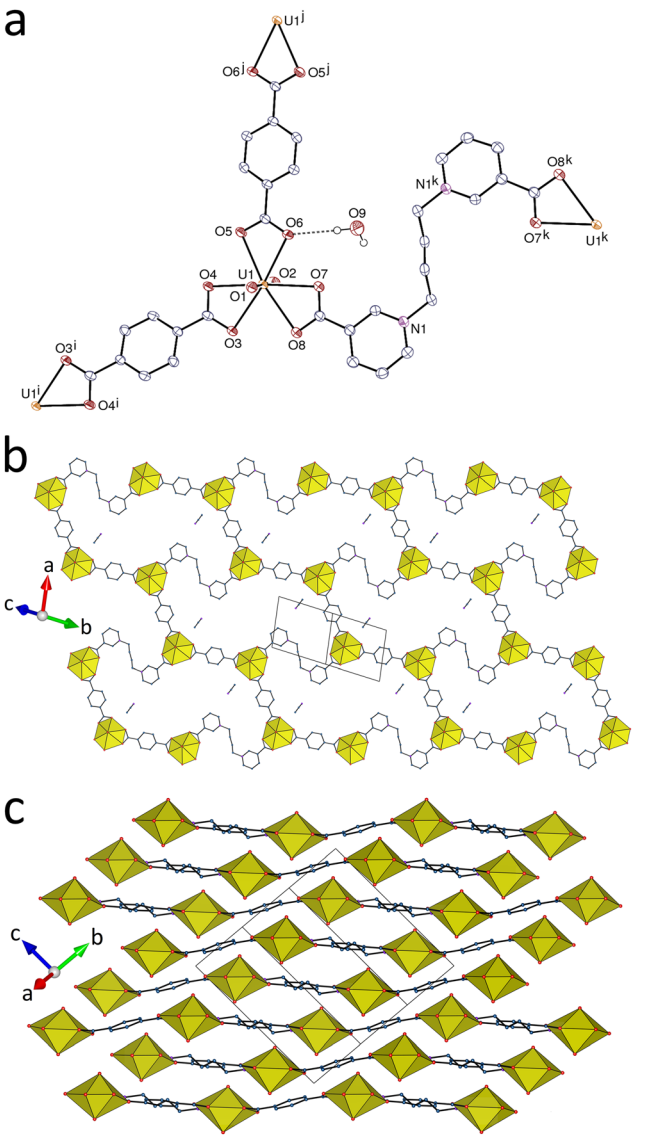

Fig. 6 (a) View of compound **6** with displacement ellipsoids shown at the 50% probability level. Carbon-bound hydrogen atoms are omitted and the hydrogen bond is shown as a dashed line. Symmetry codes: i = 1 − *x*, 2 − *y*, −*z*; j = 2 − *x*, 1 − *y*, 1 − *z*; k = −*x*, −*y*, 1 − *z*. (b) View of the **hcb** diperiodic coordination polymer with included acetonitrile molecules. (c) Packing with layers viewed edge-on and solvent excluded.

both OH⋯N (with water) and CH⋯O hydrogen bonds, thus forming links between layers. Due to the planar geometry of the sheets, the packing displays stacks of aromatic rings with parallel-displaced π–π interactions involving $ipht^{2-}$ and L2 [centroid⋯centroid distances, 3.690(2) and 3.768(2) Å; dihedral angles, 10.50(19) and 13.28(19)°; slippages, 1.23–2.08 Å], resulting in a compact arrangement (KPI, 0.72).

Using with L2 the same *t*-1,4-$chdc^{2-}$ ligand as in **3** results in the formation of the complex $[(UO_2)_2(L2)(t\text{-}1,4\text{-}chdc)_2]$ (**7**), represented in Fig. 7. The uranyl cation is κ^2*O*,*O*′-chelated by one carboxylate group from an anionic ligand and bound in monodentate fashion to two more oxygen donors from two anionic ligands and one from L2, the environment being

Open Access Article. Published on 13 January 2025. Downloaded on 11/8/2025 3:24:16 AM.
This article is licensed under a Creative Commons Attribution-NonCommercial 3.0 Unported Licence.

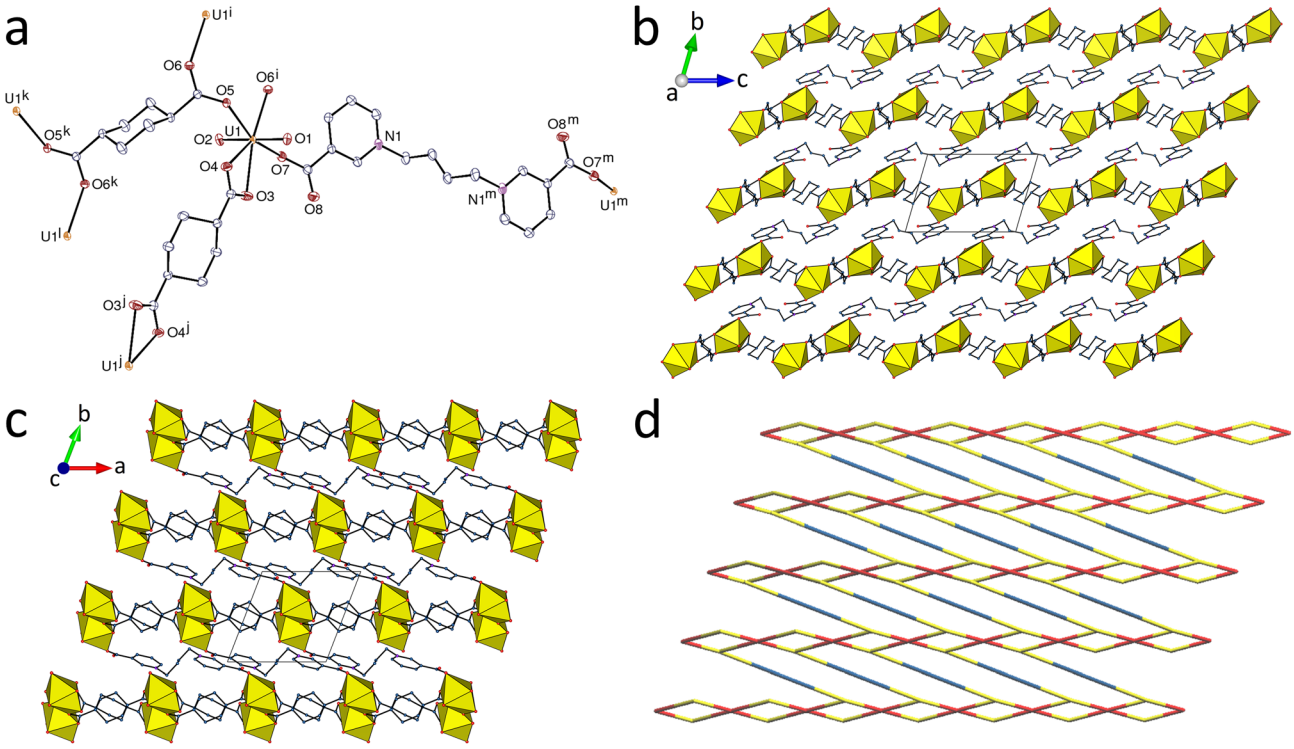

Fig. 7 (a) View of compound **7** with displacement ellipsoids shown at the 50% probability level and hydrogen atoms omitted. Symmetry codes: i = 1 − *x*, 1 − *y*, 1 − *z*; j = 2 − *x*, 1 − *y*, 2 − *z*; k = 2 − *x*, 1 − *y*, 1 − *z*; l = *x* + 1, *y*, *z*; m = −*x* − 1, 2 − *y*, 2 − *z*. (b and c) Two views of the **mog** triperiodic framework. (d) Nodal representation of the framework. U nodes, yellow; L2 edges, blue; *t*-1,4-chdc^{2-} nodes and edges, red; same orientation as in (c).

pentagonal-bipyramidal [U–O(oxo), 1.7711(18) and 1.7786(18) Å; U–O(carboxylato), 2.4367(18) and 2.4378(19) Å for the chelating group, 2.3080(18)–2.3964(17) Å for the monodentate groups]. In this case, as in **4** but without the constraints due to oxalate bonding geometry, the zwitterionic carboxylate appears to be the stronger donor (Table 2). All three ligands are centrosymmetric, the carboxylate groups of both *t*-1,4-chdc^{2-} anions being in the equatorial position and L2 assuming a divergent, kinked conformation with the two carboxylatopyridinium groups in parallel, offset planes. While the chelating *t*-1,4-chdc^{2-} ligand and L2 are simple edges, the bis(μ_2-κ^1O:κ^1O'-bridging) anionic ligand is a 4-c node, as is also the metal centre. The triperiodic, 2-nodal net formed has the $\{4.6^4{\cdot}8\}_2\{4^2{\cdot}6^2{\cdot}8^2\}$ point symbol and the unusual **mog** topological type.[42,43] The same topology was previously found in a subunit formed in a uranyl ion complex with *trans*,*trans*-muconic acid, Ni^{II} cations forming however additional edges in this case.[44] The framework in **7** contains neutral UO_2(*t*-1,4-chdc) layers which are cross-linked by the L2 ligands, the latter being too far apart from one another for π–π interactions to be present. With a KPI of 0.74, the framework does not contain solvent-accessible voids.

In complexes **1**–**6**, both zwitterionic and anionic dicarboxylates are simple edges (2-c), with both of them being bis(κ^2O,O'-chelating) in **1**–**3** and **6**. The zwitterionic ligand is bis(monodentate) in **4** and **5**, *i.e.* in the two cases in which the anionic ligand is chelating but forms a larger, 5- or 7-membered chelate ring and thus limits the available equatorial space, resulting in pentagonal-bipyramidal uranium coordination. Only in compound **7** does one of the anionic ligands become a 4-c node, resulting in an increase in periodicity and formation of a triperiodic framework (with uranium in pentagonal-bipyramidal environment). Framework formation thus appears as a direct consequence of the bis(μ_2-κ^1O:κ^1O') bridging mode adopted by one of the *t*-1,4-chdc^{2-} ligands in **7**, weak interactions and ligand flexibility probably playing a very minor role. However, an interesting point is the difference between the structures of complexes **3** and **7**, both containing *t*-1,4-chdc^{2-}, in association with L1 or L2, respectively. The former is the usual **hcb** network often associated with uranyl tris(chelation), while the latter is of the rarer $(4\text{-c})_2$ 2-nodal **mog** topology. A subtle influence of the difference in flexibility or donor strength between L1 and L2 cannot be ruled out, but is quite uncertain, as is a possible influence of the difference in organic cosolvent during the synthesis, acetonitrile for **3** and *N*,*N*-dimethylacetamide for **7**.

Luminescence properties

The photoluminescence quantum yields (PLQYs) have been measured and the emission spectra in the solid state under excitation at 420 nm have been recorded for all compounds but **4**, which could not be obtained in sufficient quantity. Complexes **1**–**3** and **7** are non-emissive (PLQY ≤ 1%) and their spectra are essentially featureless, while complex **6** is only weakly emissive (PLQY, 4%) and shows five peaks at 461, 480, 499, 522, and 545 nm (Fig. 8). In contrast, complex **5** has a rather large PLQY of 19% and its spectrum displays

Open Access Article. Published on 13 January 2025. Downloaded on 11/8/2025 3:24:16 AM.
This article is licensed under a Creative Commons Attribution-NonCommercial 3.0 Unported Licence.

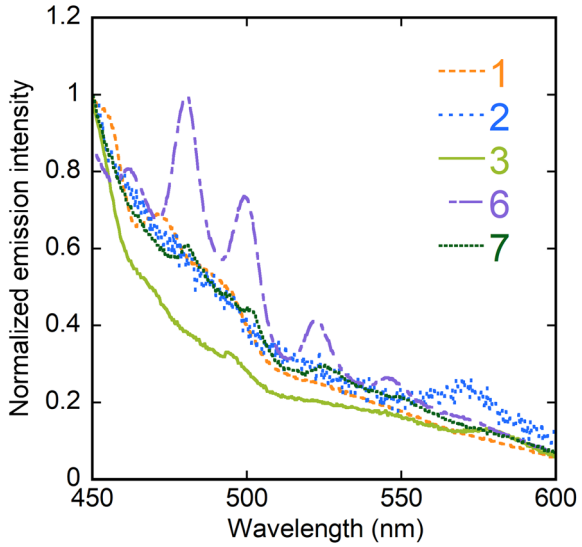

Fig. 8 Emission spectra of complexes **1**–**3**, **6**, and **7** in the crystalline state upon excitation at 420 nm.

six peaks at ~482 (shoulder), 497, 518, 542, 567, and ~594 nm (Fig. 9). Both spectra of **5** and **6** thus display the typical vibronic progression due to the $S_{10} \rightarrow S_{0v}$ (v = 0–4) transitions of the uranyl ion,[45,46] with the additional low intensity "hot-band" ($S_{11} \rightarrow S_{00}$) due to electron–phonon coupling, observed at the shortest wavelength.[47] The positions of the peaks for **5** and **6** match those usual for uranyl ion complexes with equatorial O_5 and O_6 environments, respectively.[48]

Conclusions

We have reported the synthesis and crystal structure of 7 mixed-ligand uranyl ion complexes involving a combination of zwitterionic and anionic dicarboxylates, as well as their luminescence properties in all but one case. The coordination polymers formed span the whole periodicity range, from chains, simple, daisychain or ladderlike in shape, to sheets and, in one case, a triperiodic framework. The connectivity of both types of ligands is generally low, of the 2-c, bis(monodentate) or bis(κ^2O,O'-chelating) form, with only one instance of the 4-c, bis(μ_2-κ^1O:κ^1O') bridging mode in the triperiodic framework. The anticipated difference in flexibility between ligands L1 and L2 clearly does not have a major influence on the form of their uranyl ion complexes, with mono- and diperiodic polymers being dominant for both in the present series. A contrast in behaviour is seen in the case of the two complexes obtained with 1,4-chdc^{2-} as a co-ligand, indicating perhaps that the aromatic co-ligands used in all other cases have a dominant effect due to aromatic···aromatic interactions, when present, coupled to differences in weak interactions of aromatic CH compared to aliphatic CH of 1,4-chdc^{2-}.

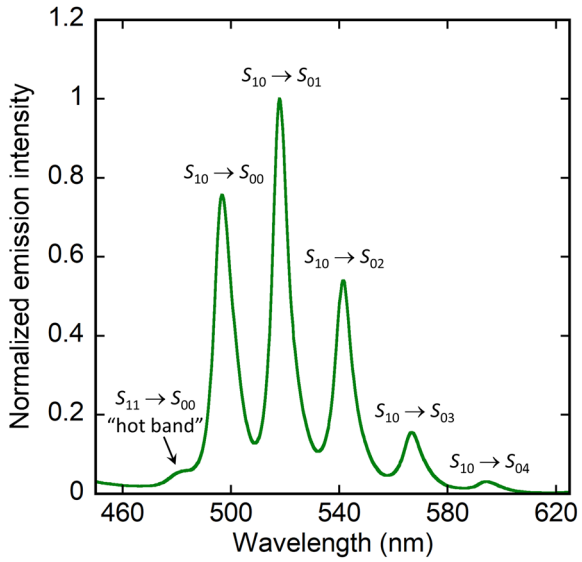

Fig. 9 Emission spectrum of complex **5** in the crystalline state upon excitation at 420 nm.

Data availability

Full structural data for the seven complexes have been deposited with the Cambridge Crystallographic Data Centre under deposition numbers 2408741–2408747. Data in cif format may be obtained at **https://www.ccdc.cam.ac.uk/structures**.

Conflicts of interest

There are no conflicts of interest to declare.

References

1 P. Thuéry and J. Harrowfield, *Coord. Chem. Rev.*, 2024, **510**, 215821.
2 P. A. Giesting and P. C. Burns, *Crystallogr. Rev.*, 2006, **12**, 205.
3 C. L. Cahill and L. A. Borkowski, in *Structural Chemistry of Inorganic Actinide Compounds*, ed. S. V. Krivovichev, P. C. Burns and I. G. Tananaev, Elsevier, Amsterdam, 2007, ch. 11.
4 T. Loiseau, I. Mihalcea, N. Henry and C. Volkringer, *Coord. Chem. Rev.*, 2014, **266–267**, 69.
5 S. Hickam and P. C. Burns, *Struct. Bonding*, 2017, **173**, 121.
6 S. Kusumoto, Y. Atoini, S. Masuda, J. Y. Kim, S. Hayami, Y. Kim, J. Harrowfield and P. Thuéry, *Inorg. Chem.*, 2022, **61**, 15182.
7 S. Kusumoto, Y. Atoini, S. Masuda, Y. Koide, K. Chainok, Y. Kim, J. Harrowfield and P. Thuéry, *Inorg. Chem.*, 2023, **62**, 7803.
8 S. Kusumoto, Y. Atoini, Y. Koide, S. Hayami, Y. Kim, J. Harrowfield and P. Thuéry, *CrystEngComm*, 2023, **25**, 5748.
9 S. Kusumoto, Y. Atoini, Y. Koide, K. Chainok, S. Hayami, Y. Kim, J. Harrowfield and P. Thuéry, *Chem. Commun.*, 2023, **59**, 10004.
10 S. Kusumoto, Y. Atoini, Y. Koide, S. Hayami, Y. Kim, J. Harrowfield and P. Thuéry, *J. Inclusion Phenom. Macrocyclic Chem.*, 2024, **104**, 209.

 This journal is © The Royal Society of Chemistry 2025

Open Access Article. Published on 13 January 2025. Downloaded on 11/8/2025 3:24:16 AM.
This article is licensed under a Creative Commons Attribution-NonCommercial 3.0 Unported Licence.

11 S. Kusumoto, Y. Atoini, S. Masuda, Y. Koide, J. Y. Kim, S. Hayami, Y. Kim, J. Harrowfield and P. Thuéry, *CrystEngComm*, 2022, **24**, 7833.
12 C. Sun, G. Xu, X. M. Jiang, G. E. Wang, P. Y. Guo, M. S. Wang and G. C. Guo, *J. Am. Chem. Soc.*, 2018, **140**, 2805.
13 J. G. Mao, H. J. Zhang, J. Z. Ni, S. B. Wang and T. C. W. Mak, *Polyhedron*, 1999, **18**, 1519.
14 *APEX4, ver. 2021.10–0*, Bruker AXS, Madison, WI, 2021.
15 *SAINT, ver. 8.40A*, Bruker Nano, Madison, WI, 2019.
16 *SADABS, ver. 2016/2*, Bruker AXS, Madison, WI, 2016.
17 L. Krause, R. Herbst-Irmer, G. M. Sheldrick and D. Stalke, *J. Appl. Crystallogr.*, 2015, **48**, 3.
18 G. M. Sheldrick, *Acta Crystallogr., Sect. A: Found. Adv.*, 2015, **71**, 3.
19 G. M. Sheldrick, *Acta Crystallogr., Sect. C: Struct. Chem.*, 2015, **71**, 3.
20 C. B. Hübschle, G. M. Sheldrick and B. Dittrich, *J. Appl. Crystallogr.*, 2011, **44**, 1281.
21 A. L. Spek, *Acta Crystallogr., Sect. C: Struct. Chem.*, 2015, **71**, 9.
22 M. N. Burnett and C. K. Johnson, *ORTEPIII*, Report ORNL-6895, Oak Ridge National Laboratory, TN, 1996.
23 L. J. Farrugia, *J. Appl. Crystallogr.*, 2012, **45**, 849.
24 K. Momma and F. Izumi, *J. Appl. Crystallogr.*, 2011, **44**, 1272.
25 V. A. Blatov, A. P. Shevchenko and D. M. Proserpio, *Cryst. Growth Des.*, 2014, **14**, 3576.
26 N. E. Brese and M. O'Keeffe, *Acta Crystallogr., Sect. B: Struct. Sci.*, 1991, **47**, 192.
27 A. L. Spek, *Acta Crystallogr., Sect. D: Biol. Crystallogr.*, 2009, **65**, 148.
28 P. Thuéry, Y. Atoini and J. Harrowfield, *Inorg. Chem.*, 2019, **58**, 6550.
29 P. Thuéry, Y. Atoini and J. Harrowfield, *Cryst. Growth Des.*, 2019, **19**, 6611.
30 P. Thuéry, Y. Atoini and J. Harrowfield, *Inorg. Chem.*, 2020, **59**, 2503.
31 J. Bernstein, R. E. Davis, L. Shimoni and N. L. Chang, *Angew. Chem., Int. Ed. Engl.*, 1995, **34**, 1555.
32 P. R. Spackman, M. J. Turner, J. J. McKinnon, S. K. Wolff, D. J. Grimwood, D. Jayatilaka and M. A. Spackman, *J. Appl. Crystallogr.*, 2021, **54**, 1006.
33 S. K. Wolff, D. J. Grimwood, J. J. McKinnon, M. J. Turner, D. Jayatilaka and M. A. Spackman, *CrystalExplorer*, University of Western Australia, 2012.
34 Y. C. Ou, R. M. Zhong and J. Z. Wu, *Dalton Trans.*, 2022, **51**, 2992.
35 P. Thuéry, *CrystEngComm*, 2008, **10**, 808.
36 M. B. Andrews and C. L. Cahill, *CrystEngComm*, 2011, **13**, 7068.
37 H. H. Li, X. H. Zeng, H. Y. Wu, X. Jie, S. T. Zheng and Z. R. Chen, *Cryst. Growth Des.*, 2015, **15**, 10.
38 P. Thuéry, Y. Atoini and J. Harrowfield, *Cryst. Growth Des.*, 2018, **18**, 3167.
39 D. E. Felton, T. A. Kohlgruber, Z. D. Tucker, E. M. Gulotty, B. L. Ashfeld and P. C. Burns, *Cryst. Growth Des.*, 2023, **23**, 8311.
40 Y. H. Lee, Y. Atoini, S. Kusumoto, S. Hayami, Y. Kim, J. Harrowfield and P. Thuéry, *Polyhedron*, 2024, **262**, 117172.
41 Y. Atoini, S. Kusumoto, Y. Koide, S. Hayami, Y. Kim, J. Harrowfield and P. Thuéry, *Polyhedron*, 2024, **250**, 116848.
42 M. O'Keeffe, M. Eddaoudi, H. Li, T. Reineke and O. M. Yaghi, *J. Solid State Chem.*, 2000, **152**, 3.
43 C. Y. Su, M. D. Smith, A. M. Goforth and H. C. zur Loye, *Inorg. Chem.*, 2004, **43**, 6881.
44 P. Thuéry and J. Harrowfield, *Inorg. Chem.*, 2022, **61**, 2790.
45 A. Brachmann, G. Geipel, G. Bernhard and H. Nitsche, *Radiochim. Acta*, 2002, **90**, 147.
46 M. Demnitz, S. Hilpmann, H. Lösch, F. Bok, R. Steudtner, M. Patzschke, T. Stumpf and N. Huittinen, *Dalton Trans.*, 2020, **49**, 7109.
47 D. H. Chen, N. Vankova, G. Jha, X. Yu, Y. Wang, L. Lin, F. Kirschhöfer, R. Greifenstein, E. Redel, T. Heine and C. Wöll, *Angew. Chem., Int. Ed.*, 2024, e202318559.
48 P. Thuéry and J. Harrowfield, *Inorg. Chem.*, 2017, **56**, 13464.